NMR Study of the Conformation and Localization of Porcine Galanin in SDS Micelles. Comparison with an Inactive Analog and a Galanin Receptor Antagonist†

Anders Öhman,‡,§ Per-Olof Lycksell,|| Anders Juréus,⊥ Ülo Langel,⊥ Tamas Bartfai,⊥ and Astrid Gräslund*,‡

Department of Biophysics and Department of Neurochemistry and Neurotoxicology, Stockholm University, Arrhenius Laboratories, S-106 91 Stockholm, Sweden, and Department of Medical Biochemistry and Biophysics, Umeå University, S-901 87 Umeå, Sweden

Received January 21, 1998; Revised Manuscript Received April 21, 1998

ABSTRACT: Galanin is a 29/30-residue neuro-endocrine peptide which performs its many important physiological functions via a membrane-bound receptor. By using two-dimensional proton NMR spectroscopy, complete relaxation matrix analysis, and simulated annealing, the conformation of porcine galanin was determined in a membrane-mimicking solvent containing sodium dodecyl sulfate (SDS) micelles. The final family of calculated structures displays three well-defined β- or γ-turn regions, comprising residues 1−5, 7−10, and 24−27, but has otherwise a random conformation. The receptor-interacting N-terminal part, residues 1−5, was found to be best defined with a backbone RMSD value of 0.12 Å. The mode of association between galanin and the SDS micelle was determined by observing the broadening effect on proton resonances, when spin-labeled 5- and 12-doxyl stearate molecules were added. It was concluded that galanin is located close to the surface of the micelle with two regions, residues 6−9 and 24−29, as well as two single residues, 18 and 21, reaching out into the aqueous solvent. Additional NMR studies were carried out on an inactive analogue, Ala^2−galanin, and an antagonist M40. The results show that the proton resonances of galanin and M40 have identical chemical shifts in the N-terminal receptor-interacting region, indicating similar solution structures in this region. For Ala^2−galanin, the same region displays a spectral heterogeneity with chemical shifts clearly different from the other two peptides, indicative of different secondary structures. These results may provide a structural background for the antagonist activity of M40 and the hormonal inactivity of Ala^2−galanin, as compared to galanin.

Galanin is a neuro-endocrine peptide (*1*) consisting of 29 amino acids (30 in humans) (*2*). It has a number of physiological functions (*3, 4*), for instance, the ability to modulate the physiological effects of insulin (*5, 6*), growth hormone (*7, 8*), acetylcholine (*9*), somatostatin (*10*), and glucagon (*10, 11*). Furthermore, the peptide has a tonic role in pain threshold control (*12*) and also an ability to stimulate feeding behavior (*13*). These biological functions are mediated by an identified membrane-bound high-affinity receptor, which is a pertussis toxin sensitive G-protein coupled glyco-protein of 54 kDa (*14*). From the cloning of the 349 amino acid human receptor protein (*15*), it is evident that it has significant homologies with other G-protein coupled receptors, which contain seven trans-membrane helices.

Porcine galanin, which is the subject of this work, is a C-terminally amidated peptide with the amino acid sequence GWTLNSAGYLLGPHAIDNHRSFHDKYGLA-NH_2. The N-terminal part has been shown to be most important for the CNS[1] receptor binding. Absolute conservation of the N-terminal 14 amino acids is also seen in all known species. The C-terminal part shows several amino acid substitutions among species, supporting the proposal that the biological activity lies in the N-terminal part. To determine the structural requirements on the peptide for biological activity, a large number of peptide fragments, chimeras, and peptides with point mutations have been synthesized and studied (*4*). Only the N-terminus is needed for full activation of hippocampal and hypothalamic galanin receptors (*16, 17*). Even a fragment comprising residues 1−12 shows a reasonable receptor binding affinity, but with a diminished activity (*18*). The most important residue is Trp^2, since substitution of this residue to Ile, Phe, Tyr, or Ala gives an essentially inactive peptide. Other important residues are Gly^1, Asn^5, and Tyr^9,

† This study was was supported by the Swedish Natural Science Research Council, the Magn. Bergvall Foundation, the Carl Trygger Foundation, the Swedish Medical Research Council, NIMH, NUTEK, and the Swedish Research Council of Engineering Sciences.

* Author to whom correspondence should be addressed.

‡ Department of Biophysics, Stockholm University.

§ Present address: Institut für Molekularbiologie und Biophysik, Eidgenössische Technische Hochschule, CH-8093 Zürich, Switzerland.

|| Department of Medical Biochemistry and Biophysics, Umeå University.

⊥ Department of Neurochemistry and Neurotoxicology, Stockholm University.

[1] Abbreviations: CNS, central nervous system; COSY, correlated spectroscopy; CD, circular dichroism; DAc, deuterated acetic acid; DOPC, 1,2-dioleoyl-*sn*-glycero-3-phosphocholine; DOPG, 1,2-dioleoyl-*sn*-glycero-3-phosphoglycerol; DQF-COSY, double quantum filtered COSY; HFP, 1,1,1,3,3,3-hexafluoro-2-propanol; MARDIGRAS, matrix analysis of relaxation for discerning the geometry of an aqueous structure; NMR, nuclear magnetic resonance; NOE, nuclear Overhauser enhancement; NOESY, nuclear Overhauser enhancement spectroscopy; RMSD, root mean square deviation; SA, simulated annealing; SDS, sodium dodecyl sulfate; TFE, 2,2,2-trifluoroethanol; TOCSY, total correlation spectroscopy; TSP, 3-(trimethylsilyl)tetradeutero sodium propionate.

S0006-2960(98)00153-6 CCC: $15.00
Published on Web 06/05/1998

which also contribute significantly to activation (*17, 19*). By substituting single or blocks of residues in rat galanin with alanine residues, it has been shown that three blocks are especially important for the binding to hypothalamic and jejunal galanin receptors (*20*). The first two blocks, residues 1−4 and 9−12, are equally important, while the third block, residues 25−29, only affects the binding to jejunal receptors. This means that the C-terminal part has the ability to distinguish between receptor subtypes.

Among the synthetic peptide analogues, a number of interesting antagonists have been found. The peptide M40, which contains the first 13 residues of galanin followed by a sequence of PPALALA, has been shown to block galanin-induced feeding (*21, 22*).

To understand the action of galanin and its analogues at a molecular level, the knowledge of the three-dimensional structures involved is important. The solution structure of galanin has been determined in 100% 2,2,2-trifluoroethanol (TFE) (*23*), using nuclear magnetic resonance (NMR) spectroscopy. In this solvent, galanin attains a well-defined structure consisting of two α-helices interrupted by a bend at the only proline residue in position 13. NMR studies on galanin in aqueous solution show that the peptide is essentially unstructured, but that residues 3−11 may adopt a nascent helix (*24*).

NMR spectroscopy has also been used to determine the solution structures of two galanin chimeras, galanin(1−12)-Ala-neuropeptide Y(25−36)-amide and galanin(1−12)-Pro-neuropeptide Y(25−36)-amide, in an aqueous solvent containing 30% 1,1,1,3,3,3-hexafluoro-2-propanol (HFP) (*25, 26*). The earlier paper described the N-terminal 12 residues, which are identical to the galanin sequence, as rather flexible with a reverse turn or a nascent helix located around Gly^8 and Tyr^9. This structural element was, however, not observed in the later study.

A mutagenesis study of the galanin receptor identified certain residues important for the interaction with galanin (*27*). Together with the previous known data from the studies of various analogues and known structures of homologous receptors and their location in a biomembrane, a model of the receptor−ligand interaction was built. In this model, Tyr^9 of galanin interacts with Phe^{282} of the receptor, which is situated close to the membrane surface. Trp^2 of galanin interacts with His^{264} and His^{267} further down in the receptor. Gly^1 was suggested to interact with Glu^{271}. A more recent study (*28*) confirms the proposed interactions between the receptor and the two residues, Trp^2 and Tyr^9, of the ligand. It is however suggested that Gly^1 of galanin most likely interacts with Phe^{115} of the receptor, instead of Glu^{271} as previously proposed.

Since the action of galanin is mediated via a membrane-bound receptor, the structure that the peptide attains, close to or in contact with membranes, should be the one which is recognized by the receptor. To mimic such an environment, vesicles, micelles, and fluorinated alcohols have been used in studies of galanin, using circular dichroism (CD) and Fourier transform infrared spectroscopy (*29*−*31*). It was shown that galanin and galanin analogues have a small amount of secondary structure in aqueous solution and in the presence of zwitterionic 1,2-dioleoyl-*sn*-glycero-3-phosphocholine (DOPC) vesicles, while negatively charged 1,2-dioleoyl-*sn*-glycero-3-phosphoglycerol (DOPG) vesicles and sodium dodecyl sulfate (SDS) micelles induce larger amount of secondary structure. Fluorinated alcohols (HFP and TFE) were shown to have the strongest influence on the structural properties of the peptides, as they stabilize the highest amount of secondary structure.

The solution structures of a number of peptides, both peptides interacting with receptors and membrane-bound peptides, have previously been determined by NMR in solutions containing SDS or dodecylphosphocholine micelles (*32*−*36*) as membrane-mimicking environments. The association of the peptide and its location relative to the micelle can be studied by adding certain paramagnetic spin-labeled fatty acids, with their nitroxide groups located at different depths inside the micelle (*32, 33, 35, 37*). The resonances of the amino acids close to the nitroxide groups are broadened beyond observation, and this can easily be seen by comparing NMR spectra in the presence and absence of spin-labels.

In the present study, two-dimensional ^1H NMR has been used to determine the conformation of galanin in a solvent containing SDS micelles. The mode of association between peptide and micelle was determined by adding appropriate spin-labels. NMR studies were also performed on the inactive analogue Ala^2−galanin, which has the essential tryptophan exchanged to an alanine, and the antagonist M40.

MATERIALS AND METHODS

Sample Preparation. Porcine galanin, Ala^2−galanin and M40 were synthesized, purified, and characterized as previously described (*38*). The peptides were dissolved in 95% H_2O/5% D_2O with 10 mM deuterated acetic acid (DAc), 150 mM deuterated sodium dodecyl sulfate (SDS), and 150 μM 3-(trimethylsilyl)tetradeutero sodium propionate (TSP), giving peptide concentrations of approximately 2.5 mM at pH 3.9 (direct meter reading). At a later stage, deuterated SDS was added to give a total concentration of 300 mM.

For the spin-label experiments, two spin-labeled fatty-acid derivatives, 5-doxyl stearate and 12-doxyl stearate, were used. These were solubilized in deuterated methanol to a concentration of 0.2 M and added to the NMR samples at a concentration corresponding to a ratio of approximately 1:60 of the SDS concentration.

DAc was purchased from Sigma, deuterated SDS from MSD ISOTOPES, Canada, TSP from Wilmad Glass Co. Inc., 5-doxyl and 12-doxyl stearate from SYNVAR, and deuterated methanol from Merck, Darmstadt.

NMR Spectroscopy. Proton NMR spectra used for resonance assignments of galanin and M40 were recorded on a Bruker AMX2-500, in a phase-sensitive mode via time-proportional phase incrementation (*39, 40*). The spectra were acquired with a spectral width of 5500 Hz and with presaturation of the water signal during the relaxation delay, 1.6−1.8 s. Double quantum filtered correlated spectroscopy (DQF-COSY) (*41*) spectra were collected with 1024 t1 increments and 2048 real data points in t2. One hundred twenty-eight transients were used in each increment. Total correlated spectroscopy (TOCSY) (*42, 43*) spectra were collected with mixing times of 60 and 75 ms, using the clean MLEV-17 mixing scheme (*44*). For M40, two additional TOCSY spectra were collected at 20 and 30 °C with a mixing time of 75 ms. The nuclear Overhauser enhancement

spectroscopy (NOESY) (*45*, *46*) spectra were recorded with mixing times of 50, 100, 150, and 200 ms.

TOCSY and NOESY spectra of galanin in a 300 mM SDS−solvent were recorded on a Varian UNITY-600 spectrometer, in a phase-sensitive mode, using the States, Ruben, and Haberkorn method (*47*). The TOCSY spectra, without and with spin-labels added, were acquired using a 60 or 75 ms clean MLEV-17 mixing sequence, a 1.5 s presaturation of the water resonance, and a spectral width of 7000 Hz. NOESY spectra, with mixing times of 100 and 150 ms, were collected for structure calculation purposes. Here, the water resonance was suppressed by the WATERGATE scheme (*48*).

For the resonance assignment of Ala^2−galanin, a number of spectra were recorded on a UNITY*plus*-600 spectrometer. The experimental setups for the TOCSY and NOESY experiment were identical to those acquired at the UNITY-600 spectrometer. In addition a DQF-COSY experiment was acquired with parameters similar to the spectrum for galanin, but with a larger spectral width of 7000 Hz.

All spectra, except when indicated, were recorded at a temperature of 25 °C. TOCSY and NOESY spectra were typically acquired with 32−48 transients, usually with 1024 real data points in t2 and 512 increments in t1.

Slowly exchanging amide protons of galanin were detected by a series of TOCSY experiments, recorded shortly after a lyophilized sample was dissolved in D_2O at pH 3.9 (direct meter reading). These TOCSY spectra were collected on a Varian UNITY-600 spectrometer, using 1024 real data points and a spectral width of 6000 Hz in the acquisition dimension and 135 increments and 3200 Hz in the indirect dimension. Six transients were collected in each increment, and a 30 ms mixing time was used.

Data Processing and Spectral Analysis. Data processing was performed with the software NMRPipe (*49*) and Felix 2.30 (Biosym Inc.), using a Silicon Graphics (SGI) or Sun workstation. TOCSY and NOESY spectra were apodized with a 75° shifted sine-bell in t2 and a 90° shifted sine-bell in t1. Prior to Fourier transformation, the time−domain data were zero-filled to 2048 points in the t2-dimension and 1024 in the t1 dimension, to give a 2048 × 1024 points data matrix in the frequency domain. A 65° shifted sine-bell was used for the DQF-COSY spectra, and the data were zero-filled to 4096 points in t2 and 2048 points in t1. For the DQF-COSY experiment of galanin this gives a digital resolution of 1.34 Hz in the frequency domain. The residual water resonance was removed from the time−domain data with a polynomial function. Baseline corrections were in the NMRPipe software achieved by applying a polynomial correction, while the base-flattening routine Flatt was used in the Felix program. Chemical shifts were in all spectra referenced to TSP.

Processed data were analyzed by the program ANSIG (*50*, *51*), running on a SGI workstation. Standard sequential assignment procedures (*52*) were used to assign the proton resonances. Cross-peak volumes in the NOESY spectra of galanin were obtained by summing up the points within an adjustable rectangular region around the cross-peak. The measured intensities for a cross-peak on each side of the diagonal were then averaged, provided that the smaller peak is larger than 50% of the other. If not, the cross-peak from the less noisy region was chosen.

Backbone NH−C^{α}H proton coupling constants were determined from the DQF-COSY spectrum, from which 1D slices of each resolved cross-peak in the fingerprint region were extracted and fitted to a double-Lorentian line shape model.

Determination of Structural Restraints. The intensities of the cross-peaks in the NOESY spectra of galanin were converted to interproton distances by using the program MARDIGRAS (*53*). This program uses the complete relaxation matrix to generate distance bounds and, therefore, it takes spin−diffusion into account. Important in this context is the rotational correlation time (τ_c) of the peptide−micelle complex. Initial runs of the MARDIGRAS program indicated an optimal τ_c of 5−5.5 ns (data not shown). A recent study shows that τ_c may be as long as 6.6 ns for a very similar peptide−micelle system of this size (*33*). To avoid biasing the result of the MARDIGRAS runs by choosing an incorrect τ_c, MARDIGRAS was run at three different τ_c, namely 5, 6, and 7 ns. The procedure for using MARDIGRAS is outlined below and follows the recommendations by the authors of the program. From an extended-chain structure of galanin and the cross-peak intensities from the NOESY spectra with mixing times of 100 and 150 ms, the program calculates distance restraints at rotational correlation times of 5, 6, and 7 ns. An absolute noise level of 0.002 is assumed, which is appropriate for a spectrum of good quality (*54*), and only fixed distances are used for the peak intensity normalization. Intraresidual distances to methyls are included with a three-step jump model. Six sets of distance restraints were calculated (one for each mixing time and rotational correlation time). Taking the extremes of the resulting restraints gave the restraints used for the initial structure determination. The program XPLOR (*55*) and the ab initio simulated annealing protocol (outlined below) were used to produce 10 structures.

On the basis of the initial structures, an additional 10 resonances could be unambiguously assigned and hence added to the structural restraints. Five of the initial structures were arbitrarily chosen as input for a second round of MARDIGRAS calculations, which produced a total of 30 sets of distance restraints. This second round, all peak intensities were used for normalization, and a three-step model was used for both intra- and interresidue methyl distances. The extremes of the resulting restraints gave the final restraints used for the following structure determination. Six lower bounds between intraresidual methyl and/or methylene groups had to be decreased to come into agreement with the covalent structure.

Dihedral Φ angle restraints were calculated from the coupling constants by using the Karplus equation (*56*), with the parameters suggested by Pardi (*57*). Each restraint extends over both solutions to the Karplus equation. A further relaxation of ±25 degrees was also included, due to the uncertainty in measuring coupling constants.

Structure Calculations. The structure calculations of galanin were performed by using the standard protocol for ab initio simulated annealing (SA) and SA refinement, as described in the XPLOR manual, version 3.0 (*55*). These protocols have a potential which represents the van der Waals interaction with a repulsive term and which does not include explicit electrostatic or hydrogen-bond potentials. Distance restraints are incorporated with a soft square-well potential

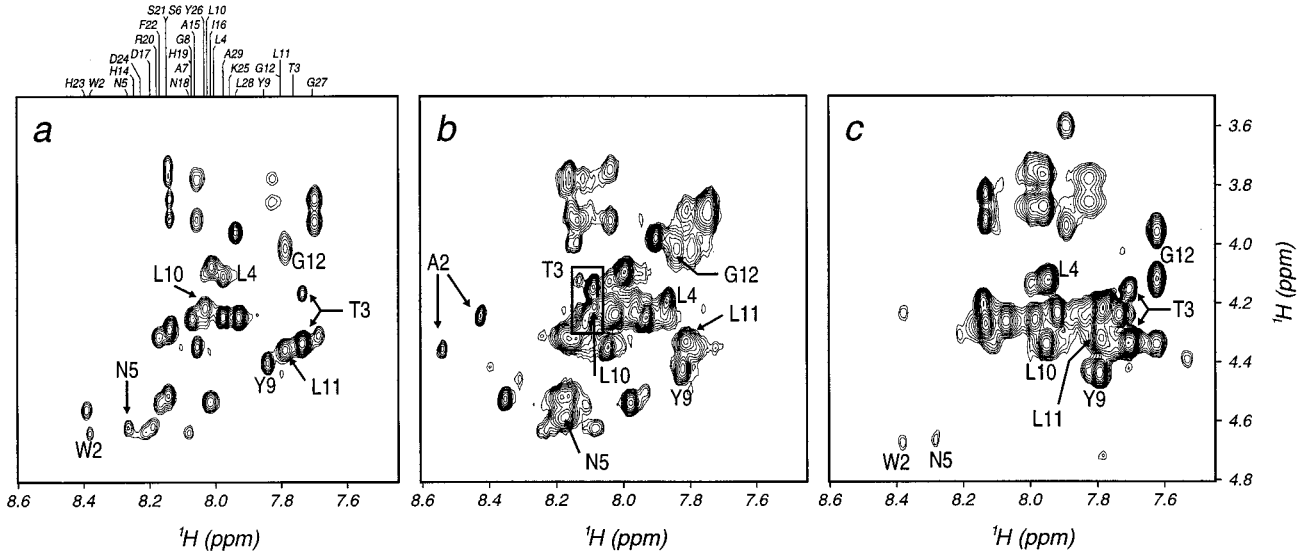

FIGURE 1: Fingerprint regions of the TOCSY spectra of galanin (a), Ala^2−galanin (b), and M40 (c). The amide proton shifts of galanin are labeled at the top of (a). Residues 2−5 and 9−12 are indicated in (a), (b), and (c) to illustrate similarities and differences between the three peptides.

in the ab initio protocol and with a square-well potential in the SA refinement protocol. A square-well potential was also used for the dihedral angle restraints. To make the calculation more stable, the time step was reduced from 5 to 3 fs. As a compensation, the duration of the protocols was increased in both protocols.

A total number of 100 structures were calculated. Each calculation started from an extended peptide conformation of good geometry. The ab initio protocol initially performs 50 steps of energy minimization followed by a 36 ps restrained molecular dynamics simulation at 1000 K. During the first two-thirds of this stage the repulsive energy is reduced, making it possible for a floating stereospecific assignment. The following annealing stage cools the system to 100 K within 18 ps, ending with 200 steps of energy minimization. Two rounds of the SA refinement protocol follow, in which the system is initially heated to 1000 K and then slowly cooled to 100 K during 21 ps, ending with 200 steps of energy minimization.

The calculated structures were partly analyzed by using the XPLOR software and partly by using the program MOLMOL (*58*). RMSD values for backbone and heavy atoms of the accepted structures were calculated with reference to an unminimized average structure in the relevant region. MOLMOL was also used to generate Figures 4 and 1S.

RESULTS

Resonance Assignments and Secondary Chemical Shifts. DQF-COSY, TOCSY, and NOESY spectra were recorded for galanin, the analogue Ala^2−galanin, and the antagonist M40 in a solvent containing deuterated SDS. Figure 1 shows the fingerprint regions of TOCSY spectra of the three peptides, recorded under similar conditions. Most of the spin systems were identified in the DQF-COSY and TOCSY spectra. These were linked together based on the information from the NOESY spectra. The aromatic residues served as good starting points together with the interresidual resonances between H^{α}-NH and H^{β}-NH protons.

All peptide samples showed weak connectivities between the H^{α} of Gly^1 and an amide proton in the same residue. These weak cross-peaks were visible only in the TOCSY but not in the NOESY spectra, and may possibly be due to the presence of an N-terminal Boc group which was not completely cleaved off during the synthesis. The presence of this minority species should not influence the structural results based on NOESY spectra. A number of very sharp cross-peaks were also observed, and they were easily identified to belong to nondeuterated SDS.

Galanin. The resonance assignments of galanin are presented as Supporting Information, Table 1S. Significant upfield shifts are noted for Lys^{25} relative to the standard random coil chemical shifts (*52*). Strong NOE connectivities are seen between H^{α} of Gly^{12} and H^{δ} of Pro^{13} (data not shown), indicative of a trans form of the proline (*52*). It should be noted that a couple of additional weak cross-peaks are observed in the fingerprint region of the TOCSY spectrum (Figure 1a; 8.03, 4.11 ppm and 7.65, 4.27 ppm). They appear close to cross-peaks assigned to Thr^3 and Leu^4, and may be due to a second minor conformer. From the peak volumes, they can be estimated to have an occupancy of less than 10% of the major conformer. No NOE's involving these resonances could be detected.

Ala^2−Galanin. The spectra of Ala^2−galanin share many of the features from the spectra of galanin, but have a number of additional cross-peak patterns together with slightly broadened resonances (Figure 1b). Partial resonance assignment showed that the N-terminal part of the peptide has two conformers, as indicated in Figure 1b, each with its individual cross-peak pattern and with significant chemical shift differences relative to galanin.

M40. Studying the spectra of M40 (Figure 1c) made it clear that there are far too many cross-peaks for a peptide of 24 amino acids, indicating that multiple conformers exist. The most likely cause for this is cis−trans isomerization of the three prolines. This explanation is also supported by the occurrence of cross-peak patterns from at least five prolines in the aliphatic region (data not shown). Changing the temperature or increasing the amount of SDS (to 300

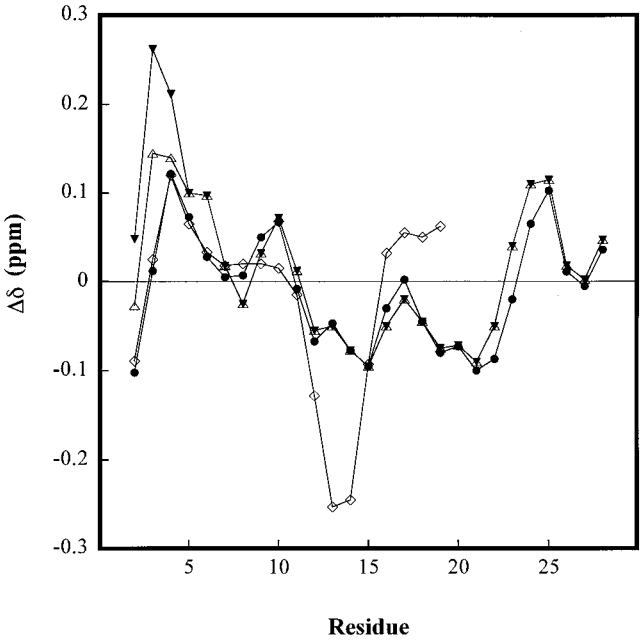

FIGURE 2: Upfield secondary chemical shifts of the C^{α} proton resonances for galanin (●), M40 (◇), Ala^2−galanin (conformer 1, △), and Ala^2−galanin (conformer 2, ▼), relative to random coil values (*59*). The chemical shifts have been averaged over three residues.

mM) did not change this situation. After partial spectral assignment it became clear that residues 1−9 have essentially the same chemical shifts as the corresponding resonances in galanin and that the variations started from residue 10. For example, compare the nonequivalent protons of Gly^{12} in M40 with the equivalent protons of Gly^{12} of galanin and Ala^2−galanin, indicated in Figure 1.

Comparison of Secondary Chemical Shifts. The chemical shift differences for a C^{α} proton resonance in a structured peptide and a random coil peptide (the secondary shift) have been shown to correlate with the secondary structure (*59*). A comparison of the secondary shifts (Figure 2) for galanin, the two conformers of Ala^2−galanin, and the major conformer of M40, shows that galanin and M40 have a striking similarity in their N-terminal part, residues 1−8, with secondary shift difference close to or below 0.01 ppm. This similarity of secondary shifts should only occur if these parts of the peptides have similar secondary structures. Residues 4 and 5 have positive secondary shifts around +0.1 ppm, indicative of a small but significant contribution of β-sheet-like secondary structure in this region. In M40, residues 12−15 have negative secondary shifts around −0.1 to −0.2 ppm, indicative of possible helical secondary structure in this region. The two conformers of Ala^2−galanin show significant secondary shift deviations from the shifts of residues 2−6 of galanin, indicating two quite different conformations as compared to galanin. The rest of the sequence has similar secondary shifts as galanin, negative for residues 12−22 and positive after residue 23. It should however be noted that there appears to be a small difference between the secondary shifts of Ala^2−galanin and galanin for residues 22−24.

Structural Restraints. An overview of the NOESY connectivities and the number of structural restraints for galanin is shown in Figure 3. The total number of NOE's are 218 of which 90 are interresidual. The first round of MARDIGRAS calculations made use of 116 intra- and 80 interresidual distance restraints, while the second round utilized 128 intra- and 90 interresidual distance restraints. The absence of long-range and only 16 medium-range connectivities suggest that the peptide as a whole does not possess a completely defined conformation.

The coupling constants of galanin, obtained from the DQF-COSY spectrum, are listed in Supporting Information, Table 1S and indicated in Figure 3a.

Structure Calculations. Of the 100 calculated structures of galanin, a total of 32 were accepted according to the following acceptance criteria: (i) RMSD for bonds, less than 0.01 Å, (ii) RMSD for angles, less than 1°, (iii) no distance violation larger than 0.5 Å, and finally (iv) no dihedral angle restraint violation larger than 5°. Gly^1 was, however, excluded from the geometric criteria, since otherwise none of the calculated structures were able to pass. This distortion can be attributed to two intense and well separated NOE's between the α-protons of Gly^1 and the amide proton of Trp^2. An overview of the structural statistics for the ensemble of accepted structures is compiled in Supporting Information, Table 2S.

Pairwise RMSD calculations show that galanin, although flexible, has three rather well-structured regions, namely those involving residues 1−5, 7−10, and 24−27. The first well-defined region, residues 1−5, has RMSD values of 0.12 and 0.48 Å for backbone and heavy atoms, respectively. Analyzing the dihedral angles of residues 1−5, (Supporting Information, Figure 1S) shows that residue 4 has a mean ψ-angle of −5° and that residue 5 has a mean ϕ-angle of 166°. This corresponds approximately to a β-turn type VII (a kink) (*60*), which ideally has $|\psi| < 60°$ and $\phi \approx 180°$.

The region involving residues 7−10 has an RMSD of 0.32 Å for the backbone and 0.56 Å for the heavy atoms, and displays a β-turn type VII conformation over residues 9 and 10. The mean ψ-angle of residue 9 is 171° and the mean ϕ-angle of residue 10 is −51°. This corresponds reasonably well with the second definition of a β-turn type VII, where the ψ-angle is $\approx 180°$ and the $|\phi| < 60°$ (as compared with the definition above) (*60*).

The C-terminal well-defined part, residues 24−27, has RMSD values of 0.26 and 0.85 Å for backbone and heavy atoms, respectively. Based on the dihedral angles, this part forms an inverse γ-turn involving residues 24−26 (*60*). The central residue, Lys^{25}, has in the accepted ensemble a mean ϕ-angle of −102°, and a mean ψ-angle of 50°, as compared with the ideal values for such a turn, covering the range of −70° to −85° for ϕ and 60° to 70° for ψ.

Figure 4a shows the backbone atoms of an ensemble of the 32 calculated structures of galanin, where the RMSD for the backbone atoms of residues 1−5 has been minimized. Figure 4b shows an enlarged view of the heavy atoms of residues 1−5, where the β-turn involving residues 4 and 5 is indicated. The β-turn over residues 9 and 10 is indicated in Figure 4c, where the heavy atoms are shown and where the RMSD for the backbone atoms of this region has been minimized. The last well-defined region, residues 24−27, is shown in Figure 4d. It displays the backbone as well as carbonyl groups and amide protons. The RMSD has been minimized for the backbone atoms.

Amide Proton Exchange. Amide proton resonances which were observable in the TOCSY spectrum 30 min after dissolving the peptide in D_2O were considered as slowly

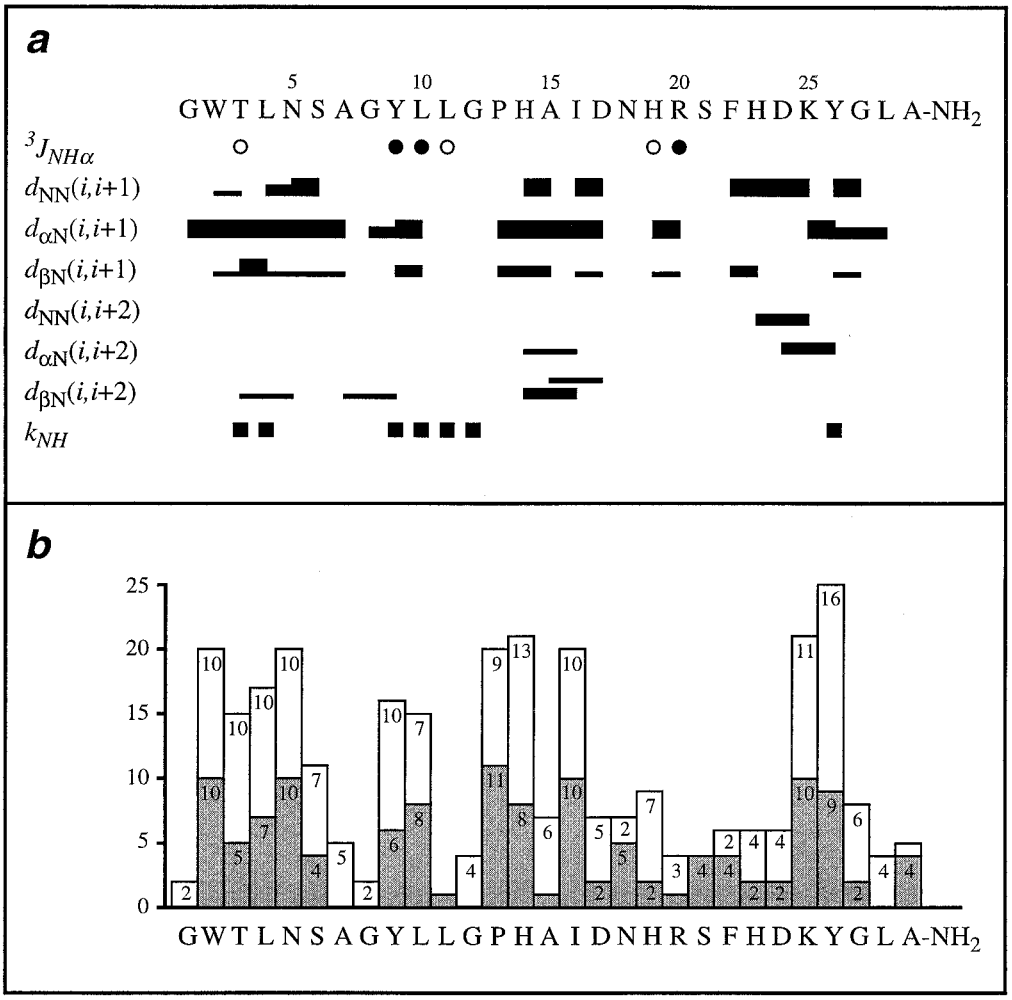

FIGURE 3: (a) The amino acid sequence of galanin, the interresidual NOE connectivities, coupling constants, and amide proton exchange rates are shown. Thick, medium, and thin bars indicate strong, medium, and weak NOE connectivities. Filled and open circles denote residues with $^3J_{NH\alpha}$ coupling constants of less than 6 Hz and larger than 8 Hz, respectively. Squares indicates amide protons which are detectable in a TOCSY spectrum 30 min after the peptide was redissolved in D_2O. (b) The diagram shows the number of intraresidual (shaded) and interresidual NOE connectivities used for the structural calculation.

exchanging. They were found in three regions of the peptide, in residues 3 and 4, residues 9−12, and residue 26, as indicated in Figure 3a.

Spin-Label Experiments. The nitroxide group of 12-doxyl stearate has previously been shown to be localized close to the center of SDS−micelles, while the nitroxide group 5-doxyl stearate is localized close to the surface of the micelle (*32, 33*). By adding each of these spin-labeled fatty-acids it is possible to probe how the peptide is located relative to the micellar surface.

Addition of 12-doxyl stearate produced a slight overall broadening of all resonances and had a minor effect on the chemical shift of His^{23} (Figure 5a and b). In contrast, 5-doxyl stearate broadened away a large fraction of all cross-peaks (Figure 5c). Two stretches of residues, 6−9 and 24−29, as well as two single residues, 18 and 21, were still observable.

DISCUSSION

Galanin is a neuro-endocrine peptide, which performs its functions via a membrane-bound receptor. Receptor−ligand interactions are normally facilitated by an initial association between the membrane and the ligand (*61, 62*). It is therefore not surprising that galanin and several of its analogues have been shown to associate with negatively charged membranes, with a concomitant secondary structure stabilization (*30, 31*).

The purpose of this NMR study was to obtain detailed structural information for galanin, its inactive analogue Ala^2−galanin, and its antagonist M40 in a membrane-mimicking solvent containing SDS micelles, and to investigate the mode of association between galanin and the micelle.

Conformation and Localization of Galanin in SDS Micelles. For galanin, complete sequential assignment and structure calculations gave rise to a structural model which has three well-defined regions, residues 1−5, 7−10, and 24−27. The best-defined region comprises residues 1−5, with a RMSD value of 0.12 Å for the backbone atoms, and includes a β-turn of type VII over residues 4 and 5 (Figure 4a and b). This well-defined region is further supported by slow amide proton exchange of residues 3 and 4 (Figure 3a). The second region, residues 7−10, has an RMSD of 0.32 Å for the backbone atoms, and displays a β-turn of type VII over residues 9 and 10 (Figure 4c). Based on the slow amide proton exchange of residues 9 to 12 (Figure 3a), a better-defined structure is expected in this region. Due to spectral overlap, only one interresidual NOE connectivity involving residues Leu^{11} and Gly^{12} could be used for the structure

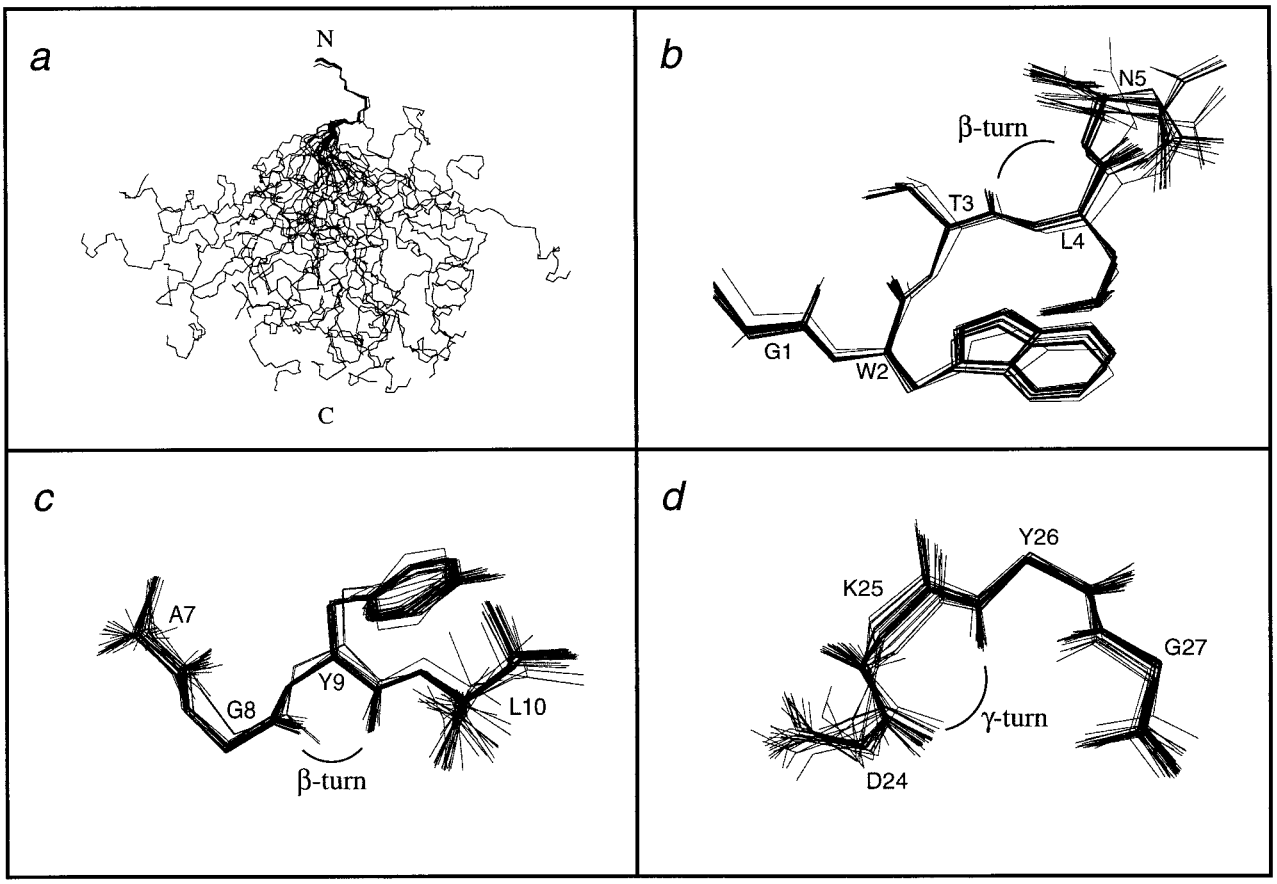

FIGURE 4: Thirty-two superimposed structures of galanin showing the (a) backbone atoms, where the RMSD for the backbone atoms of residue 1−5 has been minimized, (b) heavy atoms of residues 1−5, fitted to minimize the RMSD for these atoms, (c) heavy atoms of residues 7−10, where the RMSD for the backbone atoms have been minimized, (d) backbone as well as the carbonyl groups and amide protons of residues 24−27, and where the RMSD of the backbone atoms have been minimized. In (b), (c), and (d) the structural elements determined by the structure calculation are indicated. The figure was generated by MOLMOL (*58*).

calculation and hence accounts for the structural variability. The third region, residues 24−27, has an inverse γ-turn over Lys[25] with an RMSD of 0.26 Å for the backbone atoms (Figure 4d). Such a γ-turn involves three residues, where the amide proton of the third residue is hydrogen-bonded to the carboxyl group of the first residue. In perfect agreement, the amide proton exchange rate is slow for Tyr[26] (Figure 3a). This structural arrangement brings the aromatic side-chains of both Phe[22] and Tyr[26] into the vicinity of Lys[25] and can explain the observed upfield shifted resonances of Lys[25].

The structural model described above differs significantly from earlier studies of galanin in 100% TFE (*23*), where the peptide attained an all α-helical conformation, and in aqueous solution (*24*), where a nascent helix between residue 3−11 was found. The region containing the nascent helix does, however, coincide rather well with the region with different structural elements found in the present study. This correlation may imply that the N-terminal part of the peptide has the strongest tendency to fold.

The spin-label experiments (Figure 5) showed that no resonances were significantly broadened by the paramagnetic probe located at the center of the micelle, whereas the probe close to the micellar surface broadened most resonances except residues 6−9, 18, 21, and 24−29. These results indicate that the peptide is localized at or close to the micelle surface, with certain regions (6−9, 24−29) and single residues (18 and 21) reaching out into the aqueous solvent. It is well-known that certain amino acid residues of membrane-bound proteins are preferentially located at the surface of biomembranes. One of these is tryptophan, which is often found in the aqueous−lipid interface, functioning as an anchor (*63*). This is due to its both hydrophobic and hydrophilic character. Equally well-established is the anchor function of the positively charged amino acids, arginine and lysine (*64*, *65*). In the amino acid sequence of porcine galanin, tryptophan is found in position 2 and arginine and lysine in positions 20 and 25, respectively. The peptide has therefore three anchoring points, and it is not surprising that it is found at the micellar surface.

A schematic summary of the presence of secondary structure, well-defined structural elements, localization relative to the micelle surface and solvent accessibility reflected in amide proton exchange for each residue of galanin is given in Figure 6. Here we can observe that the N- and C-terminals have elements of β-turn secondary structure as judged from the secondary shifts. Two peptide regions, comprising residues 6−9 and 24−29, are outside the micellar surface, and approximately coincide with the structured regions, residues 7−10 and 24−27. The secondary structure of the peptide seems to be stabilized as its backbone passes through the micellar surface. The single outside residues 18 and 21 may be at the outside phase of a possible amphipathic helix, also suggested by the secondary shifts. It should however be emphasized that the structure calculation does not show this possible α-helix.

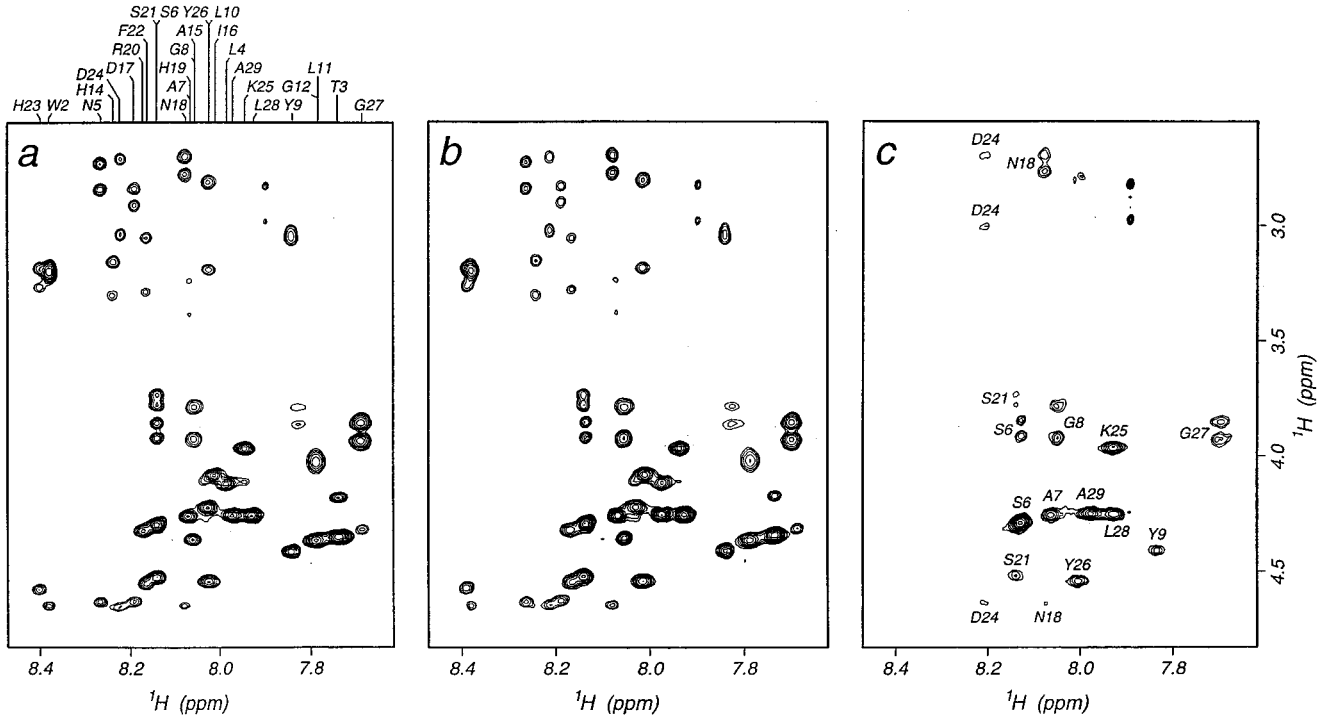

FIGURE 5: TOCSY spectra of galanin at 25 °C, in 300 mM SDS without spin-label (a), with 12-doxyl stearate added (b), and with 5-doxyl stearate added (c).

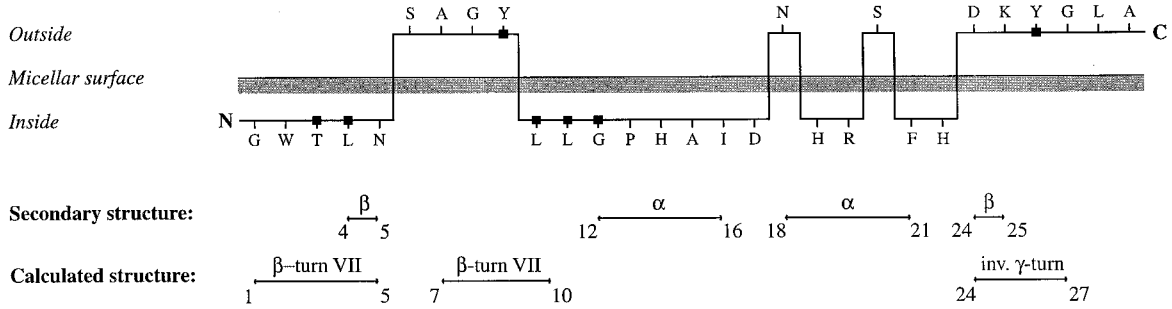

FIGURE 6: A schematic presentation of the secondary structure (judged from the secondary shifts), well-defined structural elements (determined by structure calculations), localization relative to the micelle surface (indicated by the spin-label experiments) and amide proton exchange (from the amide proton exchange experiments), for each residue of galanin. Squares indicate slowly exchanging amide protons.

Recently it was shown that the receptor binding affinity of rat galanin is mainly dependent on three regions of the peptide, namely residues 1−4, 9−12, and 25−29 (*20*). These regions coincide rather well with the structured parts found in the structure calculation, implying that these conformations may be relevant for recognition of the peptide by its CNS receptors. It should be mentioned that the two N-terminal parts of rat and porcine galanin are identical, while the C-terminal part differs (KHGLT$^{25-29}$ and KYGLA$^{25-29}$ for rat and porcine, respectively).

The localization of galanin at the water/micelle interface supports the proposed receptor interaction model (*27*, *28*). In this model the receptor residues in contact with galanin are located close to the membrane surface. In galanin, Trp^2 should be contacted just inside the surface, whereas Tyr^9 is contacted at the surface. These localizations are in agreement with our findings of localization of these residues relative to the micellar surface.

Comparison of Galanin to Ala^2-Galanin and M40. The chemical and secondary shifts (Table 1S, Figure 2) of Ala^2−galanin were found to be very similar to those for galanin, with the exception of the six N-terminal residues. Three of these (Gly^1, Ala^2, and Thr^3) actually display two sets of cross-peaks, suggesting that the exchange of Trp^2 to Ala^2 significantly alters the secondary structure in this region, and gives rise to structural heterogeneity. In a study of Gramicidin A analogues in SDS micelles, a very similar behavior was observed when tryptophan residues were exchanged to glycine or alanine (*66*). These may be other examples of the importance of tryptophan residues as membrane anchors (*63*).

In the comparison between M40 and galanin, the striking similarities of the chemical and secondary shifts of the nine N-terminal residues (Figure 2) suggest that these parts of the peptides have similar solution structures. Interestingly, it is this N-terminal part which is mainly responsible for the receptor interaction and activation. Complete sequential assignment was, however, not possible for M40 residues 10 to 20, since the spectra of M40 showed several sets of cross-peak patterns. With three prolines in this part of the sequence of M40, it is likely that these may occur in different cis/trans configurations, which leads to a number of slowly exchanging conformers.

The structural similarity between M40 and galanin in the receptor-interacting N-terminal and the corresponding dissimilarity between Ala^2−galanin and galanin provides a structural background for the antagonist activity and nonactivity of M40 and Ala^2−galanin, respectively.

ACKNOWLEDGMENT

The Swedish NMR Centre is acknowledged for the use of their Varian UNITY 600 MHz spectrometer. We thank Mrs H. Astlind for skillful processing of the manuscript.

SUPPORTING INFORMATION AVAILABLE

Table 1S shows the chemical shift assignment for porcine galanin as well as the $^3J_{NH\alpha}$ coupling constants, Table 2S gives the structural restraints and statistics (R-factors, violations, energies and rms differences) for the family of 32 porcine galanin structures, and Figure 1S gives the dihedral angles of the 32 accepted structures of galanin (3 pages). Ordering information is given on any current masthead page.

REFERENCES

1. Tatemoto, K., Rökaeus, Å., Jörnvall, H., McDonald, T. J., and Mutt, V. (1983) *FEBS Lett. 164*, 124−128.
2. Bersani, M., Johnsen, A. H., Højrup, P., Dunning, B. E., Andreasen, J. J., and Holst, J. J. (1991) *FEBS Lett. 283*, 189−194.
3. Bartfai, T., Fisone, G., and Langel, Ü. (1992) *Trends Pharmacol. Sci. 13*, 312−317.
4. Bartfai, T., Hökfelt, T., and Langel, Ü. (1993*) Crit. Rev. Neurobiol. 7*, 229−274.
5. Tatemoto, T. J., Dupre, J., Tatemoto, K., Greenberg, G. R., Radziuk, J., and Mutt, V. (1985) *Diabetes 34*, 192−196.
6. Amiranoff, B., Lorinet, A.-M., Lagny-Pourmir, I., and Laburthe, M. (1988) *Eur. J. Biochem. 177*, 147−152.
7. Bauer, F. E., Ginsberg, L., Venetikou, M., MacKay, D. J., Burrin, J. M., and Bloom, S. R. (1986) *Lancet 2*, 192−195.
8. Hulting, A.-L., Meister, B., Carlsson, L., Hilding, A., and Isaksson, O. (1991) *Acta Endocrinol. 125*, 518−525.
9. Fisone, G., Wu, C. F., Consolo, S., Nordström, Ö., Brynne, N., Bartfai, T., Melander, T., and Hökfelt, T. (1987) *Proc. Natl. Acad. Sci. U.S.A. 84*, 7339−7343.
10. Hermansen, K. (1988) *Acta Endocrinol. 119*, 91−98.
11. Lindskog, S., and Ahrén, B. (1987) *Acta Physiol. Scand. 129*, 305−309.
12. Wiesenfeld-Hallin, Z., Xu, X.-J., Langel, Ü., Bedecs, K., Hökfelt, T., and Bartfai, T. (1992) *Proc. Natl. Acad. Sci. U.S.A. 89*, 3334−3337.
13. Kyrkouli, S. E., Stanley, B. G., Hutchinson, R., Seirafi, R. D., and Leibowitz, S. F. (1990) *Brain Res. 521*, 185−191.
14. Amiranoff, B., Lorinet, A. M., and Laburthe, M. (1989) *J. Biol. Chem. 264*, 20714−20717.
15. Habert-Ortoli, E., Amiranoff, B., Loquet, I., Laburthe, M., and Mayaux, J.−F. (1994) *Proc. Natl. Acad. Sci. U.S.A. 91*, 9780−9783.
16. Fisone, G., Berthold, M., Bedecs, K., Undén, A., Bartfai, T., Bertorelli, R., Consolo, S., Crawley, J., Martin, B., Nilsson, S., and Hökfelt, T. (1989) *Proc. Natl. Acad. Sci. U.S.A. 86*, 9588−9591.
17. Land, T., Langel, Ü., Löw, M., Berthold, M., Undén, A., and Bartfai, T. (1991) *Int. J. Pept. Protein Res. 38*, 267−272.
18. Girotto, P., Bertorelli, R., Fisone, G., Land, T., Langel, Ü., Consolo, S., and Bartfai, T. (1993) *Brain Res. 612*, 258−262.
19. Amiranoff, B., Lorinet, A.-M., Yanaihara, N., and Laburthe, M. (1989*) Eur. J. Pharmacol. 163*, 205−207.
20. Juréus, A., Langel, Ü., and Bartfai, T. (1997) *J. Pept. Res. 49*, 195−200.
21. Leibowitz, S. F., and Kim, T. (1992) *Brain Res. 599*, 148−152.
22. Crawley, J. N., Robinson, J. K., Langel, Ü., and Bartfai, T. (1993) *Brain Res. 600*, 268−272.
23. Wennerberg, A. B. A., Cooke, R. M., Carlquist, M., Rigler, R., and Campbell, I. D. (1990) *Biochem. Biophys. Res. Commun. 166*, 1102−1109.
24. Morris, M. B., Ralston, G. B., Biden, T. J., Browne, C. L., King, G. F., and Iismaa, T. P. (1995) *Biochemistry 34*, 4538−4545.
25. Arvidsson, K., Land, T., Langel, Ü., Bartfai, T., and Ehrenberg, A. (1993) *Biochemistry 32*, 7787−7798.
26. Arvidsson, K., Langel, Ü., and Ehrenberg, A. (1993) *Eur. J. Biophys. 222*, 573−581.
27. Kask, K., Berthold, M., Kahl, U., Nordvall, G., and Bartfai, T. (1996) *EMBO J. 15*, 236−244.
28. Berthold, M., Kahl, U., Juréus, A., Kask, K., Nordvall, G., Langel, Ü., and Bartfai, T. (1997) *Eur. J. Biochem. 249*, 601−606.
29. Wennerberg, A. B. A., Jackson, M., Öhman, A., Gräslund, A., Rigler, R., and Mantsch, H. H. (1994) *Can. J. Chem. 72*, 1495−1499.
30. Öhman, A., Lycksell, P.-O., Andell, S., Langel, Ü., Bartfai, T., and Gräslund, A. (1995) *Biochim. Biophys. Acta 1236*, 259−265.
31. Öhman, A., Davydov, R., Backlund, B.-M., Langel, Ü., and Gräslund, A. (1996) *Biophys. Chem. 59*, 185−192.
32. Papavoine, C. H. M., Konings, R. N. H., Hilbers, C. W., and Van De Ven, F. J. M. (1994) *Biochemistry 33*, 12990−12997.
33. Jarvet, J., Zdunek, J., Damberg, P., and Gräslund, A. (1997) *Biochemistry 36*, 8153−8163.
34. Brown, L. R. (1979) *Biochim. Biophys. Acta 556*, 135−148.
35. Brown, L. R., Braun, W., Kumar, A., and Wüthrich, K. (1982) *Biophys. J. 37*, 319−328.
36. Lee, K. H., Fitton, J. E., and Wüthrich, K. (1987) *Biochim. Biophys. Acta 911*, 144−153.
37. Brown, L. R., Bösch, C., and Wüthrich, K. (1981) *Biochim. Biophys. Acta*, 556, 296−312.
38. Langel, Ü., Land, T., and Bartfai, T. (1992) *Int. J. Pept. Protein Res. 39*, 516−522.
39. Redfield, A. G., and Kunz, S. D. (1975) *J. Magn. Reson. 19*, 250−254.
40. Marion, D., and Wüthrich, K. (1983) *Biochem. Biophys. Res. Commun. 113*, 967−974.
41. Rance, M., Sørensen, O. W., Bodenhausen, G., Wagner, G., Ernst, R. R., and Wüthrich, K. (1983) *Biochem. Biophys. Res. Commun. 117*, 479−485.
42. Braunschweiler, L., and Ernst, R. R. (1983) *J. Magn. Reson. 53*, 521−528.
43. Bax, A., and Davis, D. G. (1985) *J. Magn. Reson. 65*, 355−360.
44. Levitt, M. H., Freeman, R., and Frenkiel, T. (1982) *J. Magn. Reson. 47*, 328−330.
45. Jeener, J., Meier, B. H., Bachmann, P., and Ernst, R. R. (1979) *J. Chem. Phys. 71*, 4546−4553.
46. Kumar, A., Wagner, G., Ernst, R. R., and Wüthrich, K. (1981) *J. Am. Chem. Soc. 103*, 3654−3658.
47. States, D. J., Haberkorn, R. A., and Ruben, D. J. (1982) *J. Magn. Reson. 48*, 286−292.
48. Piotto, M., Saudek, V., and Sklenár, V. (1992) *J. Biomol. NMR 2*, 661−665.
49. Delaglio, F., Grzesiek, S., Vuister, G., Zhu, G., Pfeifer, J., and Bax, A. (1995) *J. Biomol. NMR 6*, 277−293.
50. Kraulis, P. J. (1989) *J. Magn. Reson. 24*, 627−633.
51. Kraulis, P. J., Domaille, P. J., Campbell-Burk, S. L., van Aken, T., and Laue, E. D. (1994) *Biochemistry 33*, 3515−3531.
52. Wüthrich, K. (1986) *NMR of proteins and nucleic acids*, John Wiley & Sons, New York.
53. Borgias, B., and James, T. L. (1990) *J. Magn. Reson. 87*, 475−487.
54. Liu, H., Spielmann, H. P., Ulyanov, N. B, Wemmer, D. E., and James, T. L. (1995) *J. Biomol. NMR, 6*, 390−402.

55. Brünger, A. T. XPLOR manual (Version 3.0), Yale University, New Haven.
56. Karplus, M. (1959) *J. Chem. Phys. 30*, 11−15.
57. Pardi, A., Billeter, M., and Wüthrich, K. (1984) *J. Mol. Biol. 180*, 741−751.
58. Koradi, R., Billeter, M., and Wüthrich, K. (1996) *J. Mol. Graphics 14*, 51−55.
59. Wishart, D. S., Sykes, B. D., and Richards, F. M (1991) *J. Mol. Biol. 222*, 311−333.
60. Creighton, T. E. (1993) *Proteins: Structures and Molecular Properties*, W. H. Freeman and Co., New York.
61. Kaiser, E. T., and Kézdy, F. J. (1987) *Annu. Rev. Biophys. Biophys. Chem. 16*, 561−581.
62. Moroder, L., Romano, R., Guba, W., Mierke, D. F., Kessler, H., Delporte, C., Winand, J., and Christophe, J. (1993) *Biochemistry 32*, 13551−13559.
63. Schiffer, M., Chang, C.-H., and Stevens, F. J. (1992) *Protein Eng. 5*, 213−214.
64. von Heijne, G. (1989) *Nature 341*, 456−458.
65. Nilsson, I. M., and von Heijne, G. (1990) *Cell 62*, 1135−1141.
66. Hinton, J. F., Washburn-McCain, A. M., Snow, A., and Douglas, J. (1997) *J. Magn Reson. 124*, 132−139.

BI980153N